

Rapid Flu Diagnosis Using Silicon Nanowire Sensor

Fangxia Shen,^{†,#} Jindong Wang,^{‡,§,#} Zhenqiang Xu,[†] Yan Wu,[†] Qi Chen,[†] Xiaoguang Li,^{||} Xu Jie,^{||} Lidong Li,[§] Maosheng Yao,^{*,†} Xuefeng Guo,^{*,‡,⊥} and Tong Zhu^{*,†}

[†]State Key Joint Laboratory of Environmental Simulation and Pollution Control, College of Environmental Sciences and Engineering, Peking University, Beijing 100871, China

[‡]Center for Nanochemistry, Beijing National Laboratory for Molecular Sciences, State Key Laboratory for Structural Chemistry of Unstable and Stable Species, College of Chemistry and Molecular Engineering, Peking University, Beijing 100871, China

[§]School of Materials Science and Engineering, University of Science and Technology Beijing, Beijing 100083, China

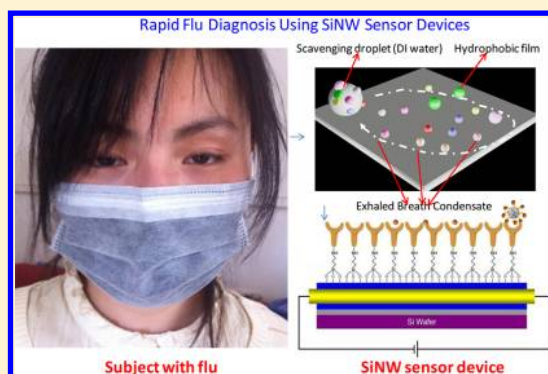
^{||}Department of Infectious Diseases, Peking University Third Hospital, Peking University, Beijing 100191, China

[⊥]Department of Advanced Materials and Nanotechnology, College of Engineering, Peking University, Beijing 100871, China

Supporting Information

ABSTRACT: Influenza epidemics worldwide result in substantial economic and human costs annually. However, rapid and reliable flu diagnosis methods are significantly lacking. Here we have demonstrated the selective detection of influenza A viruses down to 29 viruses/ μL in clinical exhaled breath condensate (EBC) samples (diluted by 100-fold) within minutes using silicon nanowire (SiNW) sensor devices. For 90% of the cases, we have observed that EBC samples tested positive or negative by gold standard method RT-qPCR generated corresponding positive or negative SiNW sensor responses. High selectivity of SiNW sensing was also demonstrated using H1N1 viruses, 8 iso PGF 2a, and inert nanoparticles. Finally, magnetic beads were shown capable of enhancing SiNW sensing directly for low level viruses and 8 iso PGF 2a. When calibrated by virus standards and EBC controls, our work suggests that the SiNW sensor device can be reliably applied to the diagnosis of flu in a clinical setting with 2 orders of magnitude less time compared to the gold standard method RT-qPCR.

KEYWORDS: Influenza A H3N2 virus, exhaled breath condensate, silicon nanowire, flu diagnosis, RT-qPCR



According to World Health Organization, annual influenza (mostly H3N2 and H1N1) epidemics worldwide are responsible for three to five million cases of severe illness, eventually leading to 250 000 to 500 000 deaths.¹ For diagnosis of viral infections, the health professionals empirically rely on the white blood cell (WBC) levels from a routine blood test and accompanying clinical symptoms such as headache, cough, and arthralgia.¹ However, this practice lacks the scientific evidence. In certain cases, RT-qPCR, regarded as the gold standard method, was employed for viral detection in nasal swabs and bronchoalveolar lavages, exhibiting higher detection rates than culturing and immuno-detection methods.^{2,3}

On another front, use of exhaled breath condensate (EBC) is attracting great attention for diagnosis of diseases owing to its completely noninvasive feature and ease of collection. Among many other compounds,^{4–6} influenza and papilloma viruses were also detected in EBC samples by RT-qPCR and ELISA methods.^{7–10} However, in addition to the false-negatives for low level influenza viruses,¹¹ the RT-qPCR method, which involves RNA extraction and amplification, takes a longer time of up to several hours for detection. Accordingly, it is not practical in a clinical setting given the large number of hospital

visits and the patient's limited wait time, especially during an influenza outbreak.

Nanotechnology-based approaches such as gold nanoparticles,¹² carbon nanotubes,¹³ quartz crystal microbalance (QCM) immunosensor,¹⁴ and silicon nanowire (SiNW)^{15–20} emerge as general platforms for label-free and ultrasensitive virus detection. Among the technologies, the SiNW field effect transistor, when chemically modified using an antibody, was shown to be able to selectively detect single influenza viruses in liquids.¹⁶ Integrated with an air sampling device and a microfluidic channel, the SiNW sensor device was also demonstrated to be able to detect airborne influenza A H3N2 viruses within minutes.²⁰ In addition to virus detection, the SiNW device has also been employed in detecting cancer biomarkers^{21,22} and human cardiac troponin-T (cTnT),²³ in some cases coupled with a built-in sample purification step.²² Yet, no studies were carried out to apply the SiNW device to

Received: April 23, 2012

Revised: June 18, 2012

Published: June 25, 2012

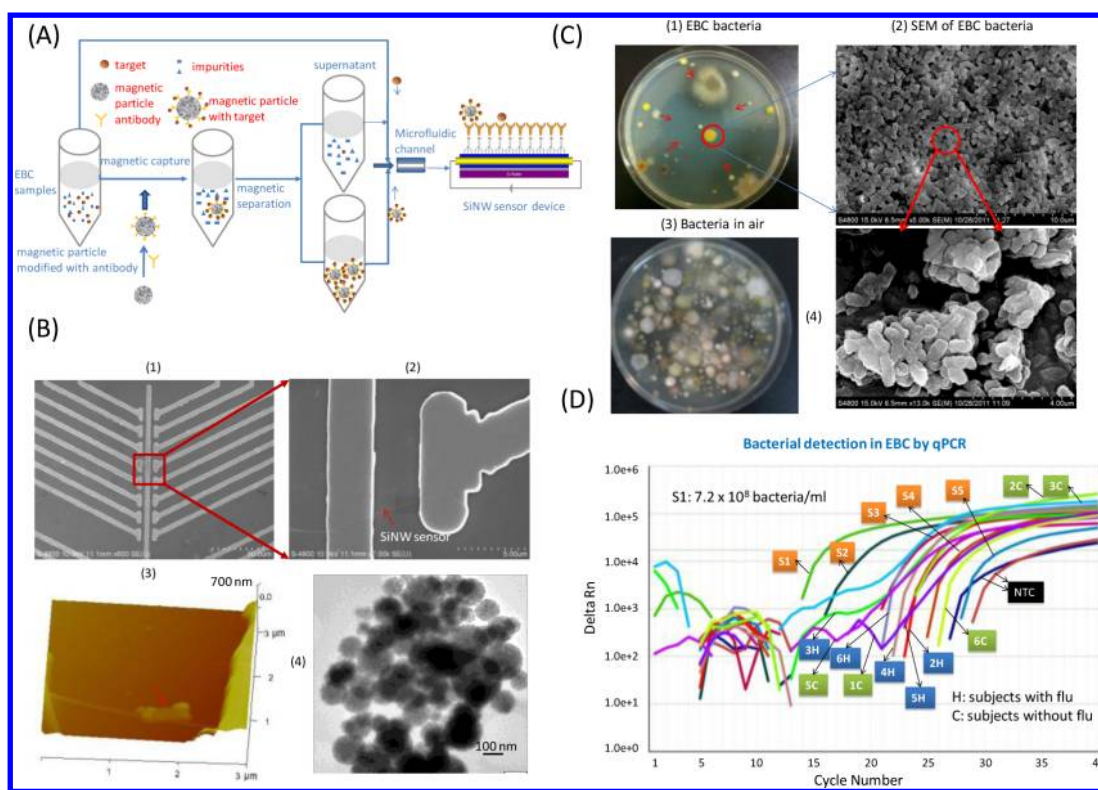


Figure 1. (A) Experimental procedure of virus and 8 iso PGF 2a detection in EBC samples using the SiNW sensor device with and without the magnetic concentrating; EBC samples collected were diluted 100-fold and transported to the sensor device at a flow rate of 170 $\mu\text{L}/\text{min}$. (B) SiNW sensor device used for the sensing experiments: (1) Optical image of the chip device, (2) SEM image of single SiNW sensor device, (3) AFM image of H3N2 virus antibody modified SiNW device together with viruses, (4) SEM images of magnetic beads. (C) Bacteria present in EBC samples collected from the human subjects with and without flu and in the indoor air: (1) bacteria in EBC samples after culturing, (2) SEM images of bacteria present in EBC samples after culturing using liquid-broth, (3) bacteria present in indoor air samples after culturing, (4) higher resolution of SEM images of bacteria present in EBC samples shown in (2). (D) Detection of bacteria in EBC samples collected from the flu subjects and nonflu subjects using qPCR.

detecting viruses in exhaled breath sample despite of the appeal of both technologies as discussed.

Here, we have successfully demonstrated the direct and selective detection of influenza viruses (H3N2) using the SiNW sensor within minutes in diluted exhaled breath condensate samples collected from the flu patients. Our data were further confirmed with the RT-qPCR tests, showing stronger PCR signals of EBC samples corresponded to higher SiNW sensor responses. Use of magnetic beads was further shown to enhance SiNW sensing for low level viruses and biomarkers. Our work has demonstrated the promise of the SiNW sensor device, when calibrated with standards and controls, for rapid diagnosis of respiratory viral infections in a clinical setting.

Materials and Methods. Experimental Procedure and Exhaled Breath Condensate (EBC) Collection. In this study, SiNW sensor devices were fabricated using chemical vapor deposition (CVD) method and applied to detecting influenza viruses including H3N2, H1N1 subtypes, and 8 iso PGF 2a biomarker in exhaled breath condensates (EBC). As shown in Figure 1A, EBC samples were first collected from human subjects with and without flu symptoms (their clinical conditions are listed in Supporting Information Table S1). The collected EBC samples were further diluted for different experiments. For some sensing experiments, diluted (100-fold) EBC samples were directly delivered to the SiNW device via a microfluidic channel at a flow rate of 170 $\mu\text{L}/\text{min}$. For other experiments, diluted EBC sample spiked with viruses or 8 iso

PGF 2a was first treated by a sample concentration and purification process using antibody modified magnetic beads, then followed by the same sensing experiments. The synthesis of SiNW device, sensor array, and polydimethylsiloxane (PDMS) were described in Supporting Information. The procedure for collecting exhaled breath condensates from human subjects is described in details in Supporting Information.

Virus Samples, 8 iso PGF 2a and Magnetic Beads. The influenza A H3N2 (1.7×10^4 viruses/ μL ; 4.6×10^4 viruses/ μL) and H1N1 virus (1.05×10^5 viruses/ μL) standards were obtained from Jiangsu Center for Diseases Prevention and Control (Jiangsu, China). The standards were serially diluted. Superparamagnetic silica magnetic beads (450 nm, 185 nm, $\sim 1 \mu\text{m}$) with a concentration level of up to 6.5×10^{17} mol Fe/ml were purchased from Allrun Nano Science and Technology Co., Ltd., Shanghai, China. The 8 iso PGF 2a standards were obtained from a kit (Groundwork Biotechnology Diagnosticate, Ltd., San Diego, California), and the standards (125 pg/mL) were also serially diluted.

Silicon Nanowire (SiNW) Device Surface Modification and Characterization. In this study, the SiNW field effect transistor sensor device shown in Figure 1B was configured following the procedure as described in Supporting Information. The electrical properties of a representative SiNW were analyzed using a semiconductor property analyzer (4156C, Agilent). The SiNW sensing devices were further functionalized using

influenza A H3N2 or H1N1 subtype antibodies (Jiangsu Center for Diseases Prevention and Control, Jiangsu, China) and 8 iso PGF 2a antibodies using the procedures detailed in our previous study.²⁰ First, the nanowire devices were treated with 5% glutaraldehyde at pH = 8 at room temperature for 1 h and then washed with phosphate buffer (10 mM, pH = 8) for 5 min. Second, the aldehyde-terminated SiNW surfaces were covalently linked with the influenza A H3N2 subtype antibody (0.1 mg/mL antibody in 10 mM phosphate buffer solution, pH = 8, containing 4 mM sodium cyanoborohydride), 8 iso PGF 2 or H1N1 antibody at 4 °C overnight (about 14 h). Before use, the SiNW devices were washed by phosphate buffer (10 mM, pH = 8) for 5 min. Unreacted aldehyde surface groups were subsequently passivated by reaction with trin-propylamine (100 mM trin-propylamine in 10 mM phosphate buffer, pH = 8) in the presence of 4 mM cyanoborohydride for 2 h. Lastly, the SiNW devices were washed using phosphate buffer (10 mM, pH = 8) for another 5 min before virus sensing experiments. Atomic force microscope (AFM) and scanning electron microscope (SEM) were used to characterize the SiNW sensor devices before and after the antibody modifications.

Virus and 8 iso PGF 2a Concentrating Using Magnetic Beads. First, the superparamagnetic silica magnetic particles of different sizes (180 nm, 450 nm, and 1 μ m) were treated with 77.6 mM 3-aminopropyl-triethoxysilane containing absolute methanol, acetic acid, and deionized water, then the supernatant was removed after a magnetic separation step. Second, the amino-terminated silica beads reacted with 5% glutaraldehyde at pH = 8 under room temperature for 1 h, then the supernatant was removed again after a second magnetic separation step. Third, the aldehyde-terminated silica beads were covalently linked with influenza A H1N1/H3N2 subtype antibody (0.01 mg/mL antibody in 10 mM phosphate buffer solution, pH = 8, containing 4 mM sodium cyanoborohydride) or 8 iso PGF 2a at 4 °C overnight (about 14 h), then the supernatant was taken out after another magnetic separation step. Before use, the silica magnetic beads also reacted with trin-propylamine (100 mM trin-propylamine in 10 mM phosphate buffer) to passivate the unreacted aldehyde surface groups in the presence of 4 mM cyanoborohydride for 2 h. Finally, the functionalized silica beads were employed for concentrating viruses and biomarker for the subsequent SiNW sensing in this study.

H3N2 Virus and 8 iso PGF 2a Detection Experiments. Before the experiments, virus samples were serially diluted and used as the standards. To investigate the influences of EBC compositions on the virus sensing experiments, viruses with different concentration levels were spiked into diluted (100-fold) EBC samples that were collected from the subjects without flu symptoms or indoor air samples taken using a BioStage impactor (SKC) (849 L air into 22.5 mL DI water). The spiked virus samples were subjected to the detection by the SiNW sensor. Following these experiments, EBC samples collected from different human subjects with and without flu symptoms (total 19) were diluted 100-fold and transported to the virus antibody modified SiNW sensor device directly via an inlet and an outlet in the polydimethylsiloxane (PDMS) channel shown in Figure 1A. The PDMS channel was placed on the sensor chip covering the entire nanowire sensor area (~4 μ m wide). The SiNW device conductance data versus time were recorded using a preamplifier (LI-76, NF Corporation) and a lock-in amplifier (LI 5640, NF Corporation), and further

displayed in a real-time manner using a LabView computer program. The lock-in amplifier was operated with a modulation frequency of 79 Hz, and the preamplifier had a current/voltage gain factor of 10^4 . The SiNW sensor device was operated with a source-drain voltage of 50 mV (OSC out (AC) as provided by the lock-in amplifier) with a reference frequency of 79 Hz. Before the sample detection, the SiNW devices were also calibrated using virus standards and EBC controls. To investigate the specific binding, 8 iso PGF 2a antibody modified SiNW device was employed to detect 8 iso PGF 2a against influenza H3N2 viruses with different concentrations following the same procedure.

In addition to the direct detection experiments using EBC samples, magnetic beads were also used to concentrate and purify viruses and 8 iso PGF 2a that were spiked into the EBC samples. The concentrating efficiencies of the magnetic beads for viruses and 8 iso PGF 2a were studied using RT-qPCR and SiNW sensor device, respectively. Following the same experimental procedure, magnetic beads with captured viruses or 8 iso PGF 2a were transported to the SiNW devices via the microfluidic channel at a flow rate of 170 μ L/min for relevant detection. Before the experiments, the SiNW devices were also calibrated by influenza viruses, 8 iso PGF 2a standards, and the bare magnetic beads. The conductance levels of the SiNW devices by different EBC samples were recorded using the preamplifier and the lock-in amplifier. To investigate the effects of physical touching of nanoparticles on the SiNW conductance, inert TiO₂ nanoparticles and magnetic beads with different concentration levels were also flown through the nanowire sensor device and the conductance levels were compared with those observed for corresponding virus and 8 iso PGF 2a standards.

RT-qPCR and Colloidal Gold Experiments. In addition to the SiNW sensing, the EBC samples collected were also analyzed using RT-qPCR. A 5 μ L EBC sample after 10-fold dilution without the RNA extraction step was used for RT-qPCR experiments. For comparison, the same EBC sample after the RNA extraction was also amplified using RT-qPCR. The RT-qPCR experiments for influenza A H3N2 virus samples were performed using the influenza H3N2/H1N1 detection kit (BioPerfectus Technologies, Shanghai) under the conditions described by the manufacturer: 50 °C (30 min, RT-PCR), 95 °C (5 min, hold), and [95 °C (10 s), 55 °C (40 s)]. The reaction mixture (25 μ L) included RT-PCR reaction buffer (12.5 μ L), enzyme mix (1 μ L), 4 μ L of primers (400 nM) and probe (200 nM), Rnase free H₂O (3.5 μ L), and sample RNA (5 μ L). For each EBC sample, at least two RT-qPCR reactions were performed. The virus concentrations in EBC samples were quantified when compared to the amplification curves of the corresponding virus standards. As a comparison, a colloidal gold kit (Guangzhou Wondfo Biotech Ltd., Guangzhou, China) was used to detect viruses in nasal swabs samples collected from some selected patients.

Results and Discussion. Detection of H3N2 Viruses That Were Spiked into Air Samples and Human Exhaled Breath Condensates Using the SiNW Sensor Device. The experimental procedure, the characterization of SiNW sensor device and magnetic beads (SEM images) in this study are shown in Figure 1A,B, respectively. A representative relationship between the gate voltage and the drain current of a p-type SiNW device is shown in Supporting Information Figure S1. During the EBC collection, airborne particulates including bacteria and fungi as shown in Figure 1C,D might be also collected into the EBC as

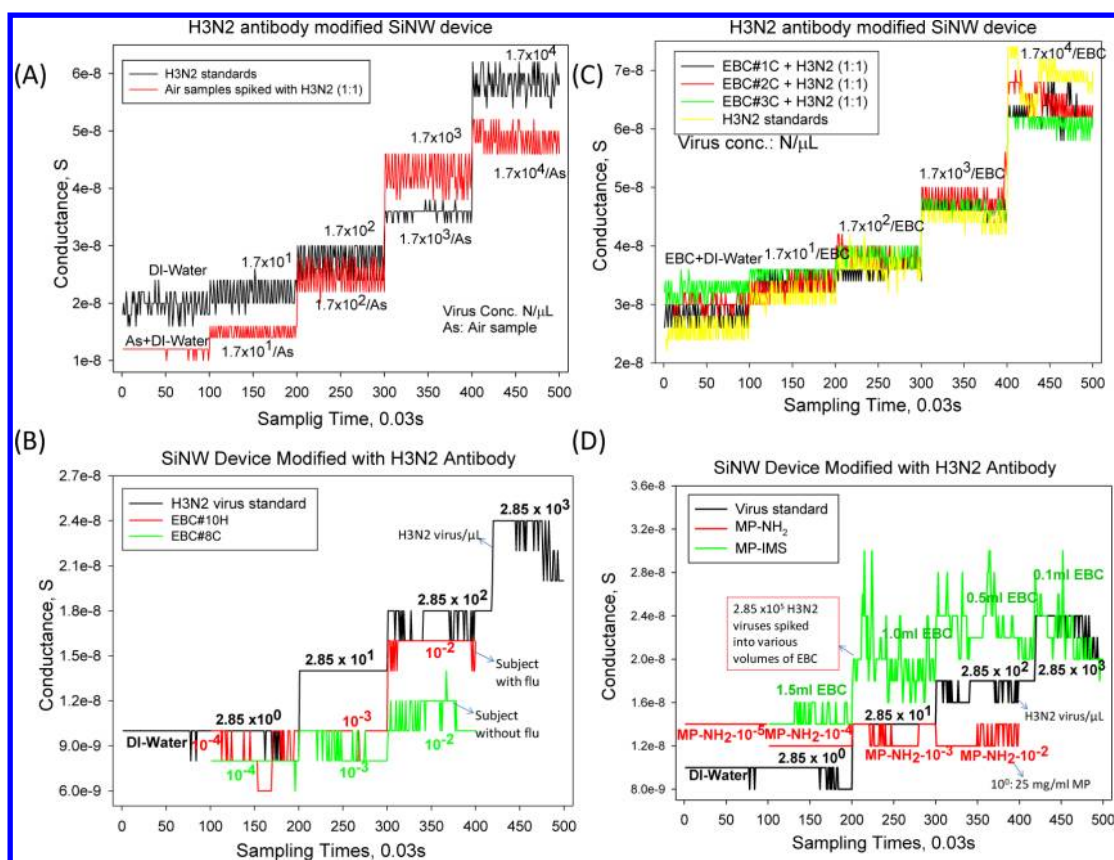


Figure 2. (A) Detection of H3N2 viruses spiked into air samples using H3N2 antibody modified SiNW device; air samples were collected from indoor environment at a flow rate of 28.3 L/min for 30 min into 22.5 mL DI water using a BioStage impactor (SKC); the H3N2 virus concentration levels were the same as those of standards except in different suspensions: air sample and DI-water. (B) Detection of H3N2 viruses in EBC samples diluted (different dilution factors: 10^{-2} , 10^{-3} , 10^{-4}) collected from one flu subject 10H and one nonflu subject. (C) Detection of H3N2 viruses with different concentration levels spiked into EBC samples (diluted 100-fold) collected from three subjects (1C–3C) without flu; virus concentrations in EBC samples were the same as those standards; nos. 1–3 refer to three different human subjects. (D) Detection of H3N2 viruses spiked into various volumes of EBC from nonflu subjects using the SiNW sensor device after the magnetic capture with a particle size of $\sim 1 \mu\text{m}$.

humans are continuously inhaling and exhaling air at an average rate of 12 L/min. This would to some extent, as observed in Figure 2A, impact virus sensing in EBC. However, as shown in Figure 2B, the influences of EBC contents such as chemicals²⁴ and microorganisms²⁵ rather than viruses decreased with increasing dilution factors (10^{-2} , 10^{-3} , 10^{-4}). When EBC samples both from the flu and nonflu subjects were diluted 1000-fold, their sensor responses were found comparable to that of DI water. Also, a 100-fold dilution for the nonflu EBC sample led to a sensor response that was lower than that of 29 viruses/ μL . In contrast, for the EBC sample from a selected flu-subject H3N2 viruses as much as 285 viruses/ μL were detected in reference to the standards after a 100-fold dilution. While minimizing the impurity influence, the 100-fold dilution of EBC was shown not to prevent the detection of low quantity of H3N2 viruses by the SiNW device due to its high sensitivity.

Similar to air sample spiking in Figure 2A, for H3N2 viruses spiked into EBC samples (diluted by 100-fold), the responses of the SiNW devices were observed to discretely increase with increasing virus concentrations (1.7×10^1 , 1.7×10^2 , 1.7×10^3 , 1.7×10^4 viruses/ μL). The H3N2 virus concentration levels shown in the figures were the same for both the EBC samples and the corresponding virus standards. In general, we have found that both for EBC and air samples that were spiked with H3N2 viruses of higher concentrations the increases in sensor response were bigger per unit fold increase in viral load as

observed in Figure 2. For EBC and air samples spiked with various levels of H3N2 viruses as low as $1.7 \times 10^3/\mu\text{L}$, their sensor responses were all observed to be greater than those EBC samples without spiking viruses. For EBC samples from the subjects without flu symptoms, comparable sensor responses were observed between the virus standards and those (the same amount) spiked into EBC samples. These results conclusively demonstrated that EBC impurities when diluted by 100-fold have minor impacts on the SiNW sensing.

Nonetheless, a concentrating step is warranted when the virus level is very low in certain cases. Here, we have demonstrated that use of H3N2 antibody-modified magnetic beads can efficiently capture and separate viruses from different volumes of EBC as observed in Figure 2D. The capture efficiency was shown to decrease with increasing volume of EBC that was spiked with the same amount (2.85×10^5 viruses) of H3N2 viruses. In addition, we have also shown that use of different loads of bare magnetic beads resulted in comparable sensor responses in contrast to discrete changes caused by the corresponding standards as shown in Figure 2D. This suggests that physical touching by magnetic beads did not cause specific sensor responses. Using an optical microscope and the SiNW sensor device, a previous study observed that physical touching only caused transient SiNW device conductance change.¹⁶ As observed in Figure 3A, our RT-qPCR tests also showed that the antibody modified magnetic

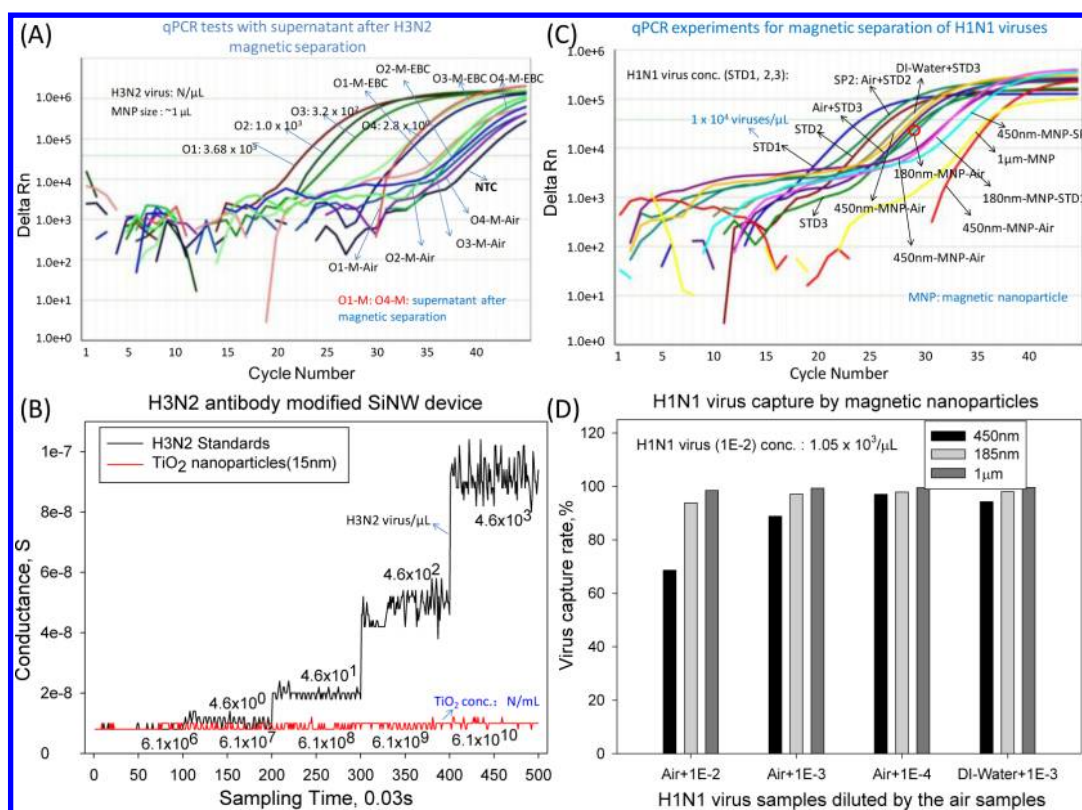


Figure 3. (A) H3N2 virus concentrating efficiencies of magnetic beads that were surface modified with H3N2 virus antibody in both air and EBC samples; EBC samples collected from subjects without flu were diluted 100-fold; “M” stands for the magnetic separation applied to air and EBC samples spiked with H3N2 viruses with concentration levels of O1, O2, and O3 as shown in the figure. (B) Effects of physical touching by inert TiO₂ nanoparticles (15 nm) with different concentration levels on the SiNW sensor response for detecting H3N2 viruses with concentration levels of 4.6×10^0 to 4.6×10^3 viruses/ μL . (C) RT-qPCR amplification curves of H1N1 virus concentrating by magnetic beads with different sizes (180 nm, 450 nm, and 1 μm) that were surface modified with H1N1 virus antibody from samples spiked with different concentration levels of H1N1 viruses; “MNP” stands for the magnetic beads. (D) RT-qPCR amplification curves of H1N1 virus concentrating efficiencies of magnetic beads with different sizes (180 nm, 450 nm, and 1 μm) surface modified with H1N1 virus antibody from samples spiked with different concentration levels of H1N1 viruses.

beads had a concentrating efficiency of more than 90% for H3N2 viruses spiked into EBC samples (1 mL). Similar to magnetic beads, use of inert TiO₂ nanoparticles of different loads, as observed in Figure 3B, was also shown not to cause specific sensor responses. Likewise, using RT-qPCR we have also observed high-concentration rate of magnetic beads for H1N1 viruses, and the efficiency was observed to increase with increasing magnetic bead size as shown in Figure 3C,D. The results from Figures 2 and 3 laid down the fundamental frame for direct virus sensing in unpurified EBC samples using the SiNW sensor device.

Detection of H3N2 Viruses in EBC Samples Collected from the Human Subjects with Flu Symptoms Using the SiNW Sensor Device. Here, the EBC samples collected from 11 human subjects (1H–11H) recruited with onset flu symptoms (listed in Supporting Information Table S1) in a respiratory clinic and 8 nonflu subjects (1C–8C) were first diluted 100-fold and then flown through the SiNW sensor device. As observed in Figure 4A,C, the EBC samples from the human subjects (C1–C8) without flu induced different sensor responses (they were close to those caused by DI water or those of low viral load of below 46 viruses/ μL), and this suggests that the physiological attributes of EBC might vary with human subjects. On the other hand, the data also suggest that nonspecific sensor responses by the EBC buffer could be higher than those caused by low level viruses in the EBC

samples. Therefore, to minimize the impact of such variations, we used 6–8 control subjects (1C–8C listed in Supporting Information Table S1) to calibrate the SiNW sensor device for all sensing experiments. For those EBC samples collected from different human subjects with onset flu symptoms, different sensor responses were also observed. Among the flu subjects, 4H and 5H samples resulted in highest H3N2 sensor responses than other four EBC samples (1H, 2H, 3H, and 6H) and nonflu subjects (1C–6C). AFM images in Figure 1B showed that there were antibodies together with viruses present on the SiNW sensor device, supporting that the conductance changes were indeed caused by the viruses. Such evidence was also obtained in a previous study using simultaneous optical and electrical observations.¹⁶

Using RT-qPCR, we have found that the EBC samples with higher SiNW sensor responses (Figure 4A) also had higher viral RNA copies as observed in Figure 4B. Here, for RT-qPCR amplification EBC samples were diluted 10-fold to minimize impurity influence. As shown in Figure 4B, 4H and 5H samples were tested H3N2 virus positive by RT-qPCR, while the control subjects (1C and 2C) were H3N2 virus negative. In reference to the H3N2 virus standards, 4H and 5H EBC samples (100-fold dilution) had H3N2 virus concentration levels of close to 4.6×10^2 viruses/ μL . For 4H and 5H EBC samples, H3N2 virus spiking (1×10^4 viruses/ μL) also resulted in positive RT-qPCR signals, which were stronger than that of the

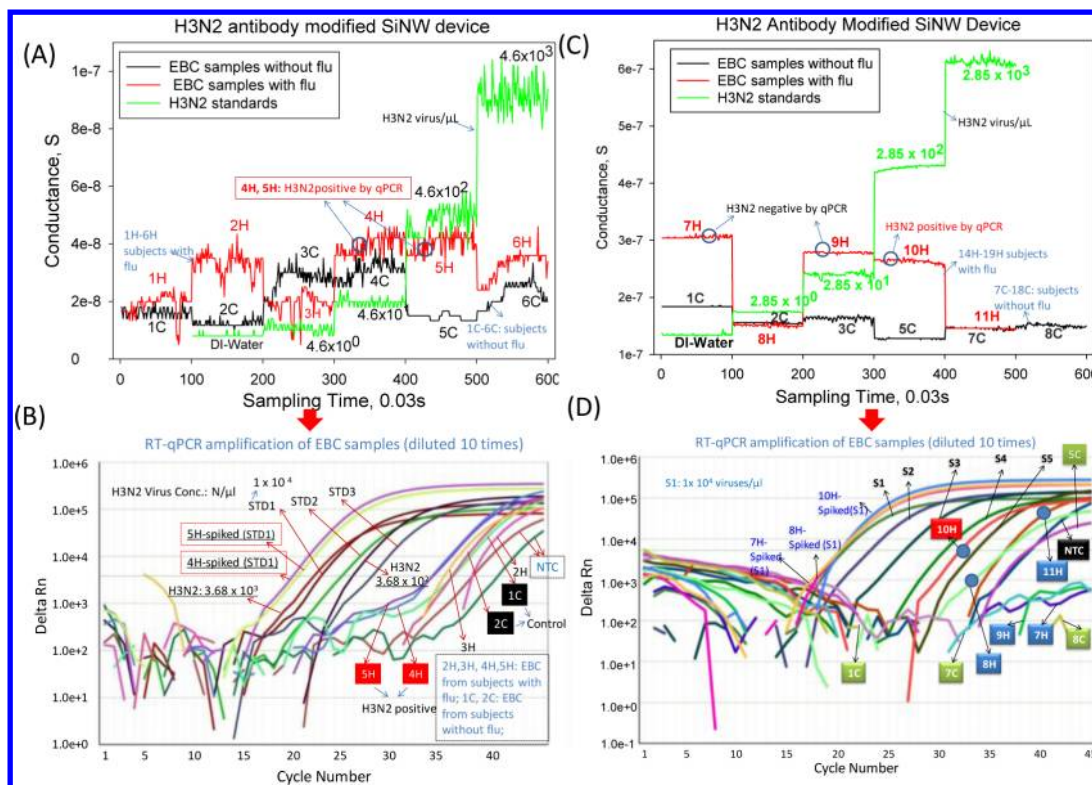


Figure 4. (A) Detection of H3N2 viruses in EBC samples (1H–6H, 1C–6C) collected from subjects with and without flu symptoms using the SiNW sensor device; EBC samples were diluted 100-fold; 1H–6H refer to subjects recruited from a hospital who had flu symptoms and their routine blood tests were listed in Table S1 (Supporting Information). (B) Detection of H3N2 viruses in EBC samples (diluted 100-fold) used in panel A using RT-qPCR: 1C–2C refer to the subjects without flu symptoms; 4H–5H refer to the subjects with flu symptoms; 4H-spiked and 5H-spiked refer to EBC samples 4H and 5H spiked with H3N2 viruses with a concentration level of 1×10^4 viruses/ μ L. (C) Detection of H3N2 viruses in EBC samples collected from the subjects (7H–11H, 1C, 2C, 3C, 5C, 7C, and 8C) with and without flu symptoms using the SiNW sensor device: a second set of experiments. (D) Detection of H3N2 viruses in EBC samples (diluted 10-fold) used in panel C using RT-qPCR; S1–S5 are serially diluted H3N2 virus standards.

spiked concentration (1×10^4 viruses/ μ L) itself. This implies that diluted EBC samples did not inhibit RT-qPCR amplification. Routine blood tests listed in Supporting Information Table S1 indicated that the human subjects corresponding to 4H and 5H EBC samples had normal white blood cell concentrations and high body temperature, which are empirically suggestive of nonbacterial infections. The corresponding sensor responses from 2H and 6H EBC samples with flu shown in Figure 4A were found in comparable levels with the control subjects (3C and 4C) without flu. RT-qPCR tests indicated that 2H and 6H were H3N2 negative (6H not shown in Figure 4B for clarity). In addition, 1H–3H, 6H were tested H1N1 negative by RT-qPCR as shown in Supporting Information Figure S2. Routine blood tests listed in Supporting Information Table S1 indicated that 2H subject had much higher white blood cell level, which is empirically suggestive of a possible bacterial infection. For subjects 1H and 3H, routine blood tests empirically suggested possible viral infections, however in our experiments their EBC samples caused lower sensor responses. There might be two possible reasons for the discrepancy: low H3N2 virus concentrations in the EBC samples from these two subjects, or other possible virus types present, which however were not tested by the SiNW device in our study (the sensor device was modified using H3N2 virus antibody). Our RT-qPCR tests (Figure 4B) also indicated that 1H and 3H were H3N2 negative (1H not shown for clarity).

To further confirm the application of the SiNW device for rapid flu diagnosis, we have performed a second set of similar experiments and the results are shown in Figure 4C,D. As observed in Figure 4C, EBC samples (diluted by 100-fold) from the nonflu subjects (1C–3C, 5C, 7C, and 8C) caused sensor responses that were close to that of DI water (equivalent to that by 3 viruses/ μ L). However, for flu subjects 7H, 9H, and 10H, their H3N2 sensor responses were observed to be much higher than other flu subjects and the virus standard of 29 viruses/ μ L. Our RT-qPCR tests showed that 10H was also H3N2 positive while 7H were H3N2 and H1N1 negative as observed in Figure 4D and Supporting Information Figure S3, respectively. However, 9H sample was shown to exhibit stronger H1N1 RT-qPCR signal than other EBC samples as observed in Supporting Information Figure S3. Thus, it is possible that the antibody could cross-react with H1N1 and H3N2, and this possibility was also shown by a recent study.²⁶ Accordingly, the discrepancy for 7H and 9H between these two technologies might be attributed to RT-qPCR amplification limitations, for example, possible inhibition and/or low quantity,¹¹ or the nonspecific binding for SiNW sensor, for example, with 9H. Routine blood test shown in Supporting Information Table S1 indicated that 7H was possibly infected with viruses. Using colloidal gold method all subjects (7H–11H) were tested influenza A negative. From these two sets of independent experiments, it was found that 90% of EBC samples tested H3N2 positive or negative by RT-qPCR also

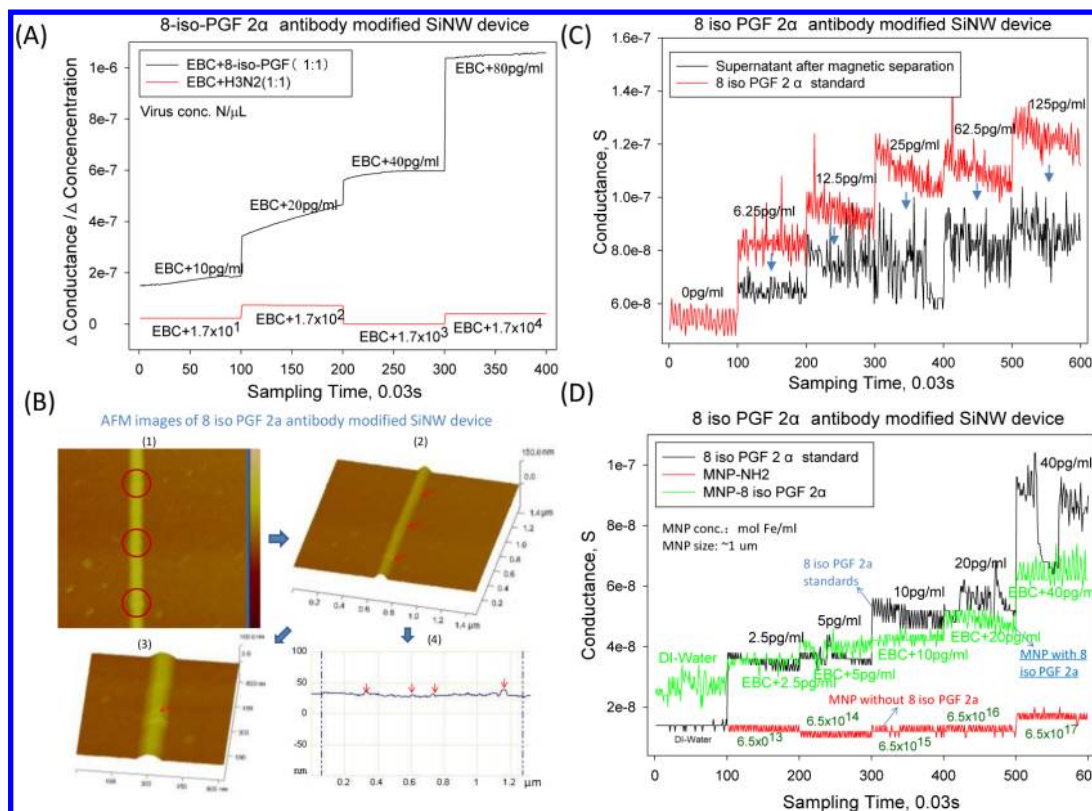


Figure 5. (A) Selective detection of 8 iso PGF 2 α against H3N2 viruses with different concentration levels; EBC samples from the subjects without flu symptoms were diluted 100-fold and spiked with H3N2 viruses and 8 iso PGF 2 α biomarker, respectively. (B) AFM images of 8 iso PGF 2 α antibody modified SiNW device: (1), (2) and (3) refer to AFM images of the antibody modified SiNW device; circle and arrow point to the 8 iso PGF 2 α antibody chemically linked to the SiNW device surface; (4) the vertical height of the antibody lined to the SiNW surface. (C) The 8 iso PGF 2 α concentrating efficiencies of magnetic beads with a size of 1 μ m surface modified with 8 iso PGF 2 α antibody from EBC spiked with different concentration levels of 8 iso PGF 2 α (0–125 pg/mL); 8 iso PGF 2 α in the supernatant after the magnetic separation was detected with the same SiNW devices. (D) Detection of 8 iso PGF 2 α biomarker with different concentration levels (2.5–40 pg/mL) spiked into EBC samples from subjects without flu using SiNW sensing device after the magnetic capture with a particle size of \sim 1 μ m.

generated corresponding positive or negative SiNW sensor responses specific for H3N2. In general, the flu viruses include three major types: Influenza virus A, Influenza virus B, and Influenza virus C. For influenza A viruses, they also include subtypes of H1N1 (caused Spanish Flu in 1918, and Swine Flu in 2009), H2N2 (caused Asian Flu in 1957), H3N2 (caused Hong Kong Flu in 1968), H5N1 (caused Bird Flu in 2004), H7N7, H1N2, H9N2, H7N2, H7N3, and H10N7. Influenza viruses A, B and C are very similar in overall structures. These viruses are made of a viral envelope containing two main types of glycoproteins, wrapped around a central core. Hemagglutinin (HA) and neuraminidase (NA) are the two large glycoproteins on the outside of the viral particles. However, these viruses have different H(A) and N(A) compositions, and antibody cross reactions do exist among certain viruses. However, extensive tests with all these subtypes including H1N1 viruses were beyond the scope of this study.

In addition to other impurities, EBC samples could also contain other biomarkers such as 8 iso PGF 2 α .²⁷ To investigate the effects of nonspecific antibody binding, we tested the SiNW device modified using 8 iso PGF 2 α antibody when detecting different loads of 8 iso PGF 2 α (10, 20, 40, and 80 pg/mL) against H3N2 viruses (1.7×10^1 , 1.7×10^2 , 1.7×10^3 , 1.7×10^4 viruses/ μ L). As observed in Figure 5A, different 8 iso PGF 2 α loads generated discrete changes in sensor responses, while those H3N2 viruses resulted in similar sensor responses regardless of concentrations (4 orders of magnitude difference).

AFM images shown in Figure 5B indicated that there were 8 iso PGF 2 α antibodies present on the surface of the SiNW device. The data from Figure 5A,B suggest that there were no specific binding between H3N2 viruses and 8 iso PGF 2 α antibody. The presence of various types of bacteria shown in Figure 1C in EBC samples from human subjects was also shown not to cause specific sensor response for virus or 8 iso PGF 2 α antibodies as no changes in conductance levels of the SiNW device were detected. Likewise, the presences of such high levels of bacteria (\sim 500 CFU/ m^3) in air samples shown in Figure 5D also had minor impacts on the SiNW sensing experiments with H3N2 viruses. In other studies, selective detection of multiple cancer biomarkers in serum samples and viruses in liquids were successfully demonstrated using the SiNW sensor array that was modified using different antibodies.^{16,21} The data from the SiNW sensing experiments, RT-qPCR and routine blood tests here conclusively suggest that the SiNW sensor device can be immediately applied to detecting influenza virus in clinical EBC samples after diluted 100-fold, and the SiNW device had similar detection rates with the gold standard RT-qPCR. However, the detection time from the EBC collection to the virus sensing using the SiNW sensor device was observed around 2 min. This time scale is substantially smaller than that of the RT-PCR method and other commercially available rapid flu diagnosis methods (limited sensitivity).²⁸

Selective Detection of H3N2, H1N1 Viruses As Well as 8 iso PGF 2 α Biomarker Captured by Magnetic Beads. To enhance

SiNW sensor response for low level virus or biomarker, more efficient EBC collection device should be developed or a concentrating step should be adopted before the SiNW detection. As discussed above, magnetic beads had higher concentrating efficiencies. In this work, we have flown the magnetic beads with captured viruses or 8 iso PGF 2a directly to the SiNW sensor device without the bioextraction step. For quality control, the SiNW sensor devices were calibrated using 8 iso PGF 2a biomarker, H3N2 viruses and the bare magnetic beads itself. Similar to H3N2 and H1N1 viruses, we observed that after the magnetic separation of 8 iso PGF 2a the supernatant had substantially lower SiNW sensor responses than those without the separation as shown in Figure 5 C. The lower sensor response was due to the decrease of 8 iso PGF 2a biomarker concentration in the same EBC buffer after the separation experiment. This, on the other hand, also supports that the changes in conductance levels of the antibody-modified SiNW sensor device were indeed caused by the specific binding of the antibody to 8 iso PGF 2a biomarker.

Previously, a microfluidic purification chip was integrated into silicon nanoribbon sensor for detecting cancer biomarker in whole blood.²¹ Here, our data shown in Figures 2D, 3C,D and 5C,D suggest that for those EBC samples with lower virus or biomarker concentrations magnetic beads can be used to concentrate them for direct detection. This is especially useful when viruses or biomarkers are in low quantities in human samples. As shown in Figure 5D, the SiNW sensor device can detect a difference of at least 6 pg/mL 8 iso PGF 2a. As also observed in the figure, regardless of their concentration levels the bare magnetic beads ($\sim 1 \mu\text{m}$) resulted in similar sensor responses, which were comparable to those caused by DI water. Similar to H3N2 virus sensing, as shown in Supporting Information Figure S3 TiO₂ nanoparticles with different loads were shown to generate similar responses from the SiNW device that was surface-modified using 8 iso PGF 2a antibodies. Interestingly, those magnetic beads with captured 8 iso PGF 2a biomarker from the same EBC suspensions were shown to result in similar sensor responses compared to the corresponding standards used for the spiking as observed in Figure 5D. These data unambiguously indicated that physical touching by the nanoparticles did not cause specific sensor responses and those magnetic beads after the separation and purification experiments with EBC samples can be used directly for the SiNW sensing. Use of magnetic beads can allow the SiNW device to directly detect low level viruses or biomarkers in a complex physiological sample.

Conclusions. For the first time, our work has demonstrated the capability of SiNW sensor devices in selectively detecting influenza viruses within minutes in clinical EBC samples collected from human subjects with onset flu symptoms. For 90% of the cases, we have observed that EBC samples tested positive or negative by the RT-qPCR method generated corresponding positive or negative SiNW sensor responses with an unparalleled speed. While for those EBC samples with very low quantity of viruses, antibody modified magnetic beads were shown capable of efficiently concentrating the viruses for direct detection by the SiNW sensor device. Variations in sensor devices were found among SiNW devices, however when calibrated by the standards and different EBC controls from nonflu subjects the relevant impacts can be minimized. Another limiting factor with the technology is the cross-reaction between antibodies and nontarget antigens which is a common problem to immuno-based detection methods. Future improve-

ment of the specific binding of antibody would greatly improve the sensing technology by SiNW devices. Although H3N2/H1N1 viruses and 8 iso PGF 2a biomarker were primarily used here, our SiNW sensor system can be certainly extended to other types of viruses or biomarkers present in EBC samples. Integration of different virus antibody modified SiNW sensor devices in a single chip using a micropipet technology would offer the opportunity to simultaneously detect different viruses in a single EBC sample. Such kind of integration has already been demonstrated in detecting multiple cancer markers in serum samples.²¹ Over the years, the SiNW device has been extensively investigated as a biosensor in various applications, and our study further moves this technology from the bench closer to the clinical bed. Commercialization of the technology described in this work as a hand-held device opens up outstanding opportunities of revolutionizing the flu diagnosis in the clinical setting.

■ ASSOCIATED CONTENT

📄 Supporting Information

Additional information and materials. This material is available free of charge via the Internet at <http://pubs.acs.org>.

■ AUTHOR INFORMATION

Corresponding Author

*(M.Y.) E-mail: yao@pku.edu.cn. Phone: +86 010 6276 7282.
(X.G.) E-mail: guoxf@pku.edu.cn. Phone: +86 01062757789.
(T.Z.) E-mail: tzhu@pku.edu.cn. Phone: +86 01062754789.

Author Contributions

[#]F.S and J.W contributed equally to the work.

Notes

The authors declare no competing financial interest.

■ ACKNOWLEDGMENTS

This study was supported by the National High Technology Research and Development Program of China (Grant 2008AA062503), MOST (2009CB623703 and 2012CB921404), National Science Foundation of China (Grants 20877004, 21077005, and 20833001), and the special fund of State Key Joint Laboratory of Environment Simulation and Pollution Control.

■ REFERENCES

- (1) World Health Organization. Influenza (seasonal) 2009. <http://www.who.int/mediacentre/factsheets/fs211/en/index.html> (accessed Dec 5, 2011).
- (2) Xiang, X. Y.; Qiu, D. W.; Chan, K. P.; Chan, S. H.; Hegele, R. G.; Tan, W. C. Comparison of three methods for respiratory virus detection between induced sputum and nasopharyngeal aspirate specimens in acute asthma. *J. Virol. Methods* **2002**, *101*, 127–133.
- (3) Chen, Y.; Cui, D. W.; Zheng, S. F.; Yang, S. G.; Tong, J.; Yang, D. G.; Fan, J.; Zhang, J.; Lou, B.; Li, X. F.; Zhuge, X. L.; Ye, B.; Chen, B. D.; Mao, W. L.; Tan, Y. J.; Xu, G. Y.; Chen, Z. J.; Chen, N.; Li, L. J. Simultaneous detection of influenza A, Influenza B, and respiratory syncytial viruses and subtyping of influenza A H3N2 virus and H1N1 (2009) virus by multiplex real-Time PCR. *J. Clin. Microbiol.* **2011**, *49*, 1653–1656.
- (4) Liu, J.; Sandrini, A.; Thurston, M. C.; Yates, D. H.; Thomas, P. S. Nitric oxide and exhaled breath nitrite/nitrates in chronic obstructive pulmonary disease patients. *Respiration* **2007**, *74*, 617–623.
- (5) Pauling, L.; Robinson, A. B.; Nishit, R. T.; Cary, P. Quantitative Analysis of urine vapor and partition chromatography breath by gas-Liquid. *Proc. Nat. Acad. Sci. U.S.A.* **1971**, *68*, 2374–2376.

- (6) Phillips, M.; Gleeson, K.; Hughes, J. M. B.; Greenberg, J.; Cataneo, R. N.; Baker, L.; McVay, W. P. Volatile organic compounds in breath as markers of lung cancer: a cross-sectional study. *Lancet* **1999**, *353*, 1930–33.
- (7) Fabian, P.; McDevitt, J. J.; DeHaan, W. H.; Fung, R. O. P.; Cowling, B. J.; Chan, K. H.; Leung, G. M.; Milton, D. K. Influenza virus in human exhaled breath: an observational study. *Plos One* **2008**, *3*, e2691.
- (8) Huynh, K. N.; Oliver, B. G.; Stelzer, S.; Rawlinson, W. D.; Tovey, E. R. A new method for sampling and detection of exhaled respiratory virus aerosols. *Clin. Infect. Dis.* **2008**, *46*, 93–95.
- (9) Turchiarelli, V.; Schinkel, J.; Molenkamp, R.; Foschino Barbaro, M. P.; Carpagnano, G. E.; Spanevello, A.; Lutter, R.; Bel, E. H.; Sterk, P. J. Repeated virus identification in the airways of patients with mild and severe asthma during prospective follow-up. *Allergy* **2011**, *66*, 1099–1106.
- (10) Carpagnano, G. E.; Koutelou, A.; Natalicchio, M. I.; Martinelli, D.; Ruggieri, C.; Taranto, A. D.; Antonetti, R.; Carpagnano, F.; Foschino-Barbaro, M. P. HPV in exhaled breath condensate of lung cancer patients. *Br. J. Cancer* **2011**, *105*, 1183–1190.
- (11) Singh, K.; Vasoo, S.; Stevens, J. Pitfalls in diagnosis of pandemic (Novel) A/H1N1 2009 influenza. *J. Clin. Microbiol.* **2010**, *48* (4), 1501–1503.
- (12) Driskell, J. D.; Jones, C. A.; Tompkins, S. M.; Tripp, R. A. One-step assay for detecting influenza virus using dynamic light scattering and gold nanoparticles. *Analyst* **2011**, *136*, 3083–3090.
- (13) Tam, P. D.; Hie, N. V.; Chien, N. D.; Le, A. T.; Tuan, M. A. DNA sensor development based on multi-wall carbon nanotubes for label-free influenza virus (type A) detection. *J. Immunol. Methods* **2009**, *350*, 118–124.
- (14) Li, D. J.; Wang, J. P.; Wang, R. H.; Li, Y. B.; Abi-Ghanem, D.; Berghman, L.; Hargis, B.; Lu, H. G. A nanobeads amplified QCM immunosensor for the detection of avian influenza virus H5N1. *Biosens. Bioelectron.* **2011**, *26*, 4146–4154.
- (15) Cui, Y.; Wei, Q. Q.; Park, H. K.; Lieber, C. M. Nanowire nanosensors for highly sensitive and selective detection of biological and chemical species. *Science* **2001**, *293*, 1289–1292.
- (16) Patolsky, F.; Zheng, G. F.; Hayden, O.; Lakadamyali, M.; Zhuang, X. W.; Lieber, C. M. Electrical detection of single viruses. *Proc. Natl. Acad. Sci. U.S.A.* **2004**, *101*, 14017–14022.
- (17) Patolsky, F.; Zheng, G.; Lieber, C. M. Fabrication of silicon nanowire devices for ultrasensitive, label-free, real-time detection of biological and chemical species. *Nat. Protoc.* **2006**, *1*, 1711–1724.
- (18) Stern, E.; Klemic, J. F.; Routenberg, D. A.; Wyrembak, P. N.; Turner-Evans, D. B.; Hamilton, A. D.; LaVan, D. A.; Fahmy, T. M.; Reed, M. A. Label-free immunodetection with CMOS-compatible semiconducting nanowires. *Nature* **2007**, *445*, 519–522.
- (19) Zhang, G. J.; Zhang, L.; Huang, M. J.; Luo, Z. H. H.; Tay, G. K. I.; Lim, E. J. A.; Kang, T. G.; Chen, Y. Silicon nanowire biosensor for highly sensitive and rapid detection of Dengue virus. *Sens. Actuators B* **2010**, *146*, 138–144.
- (20) Shen, F.; Tan, M.; Wang, Z.; Yao, M.; Xu, Z.; Wu, Y.; Wang, J.; Guo, X.; Zhu, T. Integrating silicon nanowire field effect transistor, microfluidics and air sampling techniques for real-time monitoring biological aerosols. *Environ. Sci. Technol.* **2011**, *45*, 7473–7480.
- (21) Zheng, G.; Patolsky, F.; Cui, Y.; Wang, W.; Lieber, C. M. Multiplexed electrical detection of cancer markers with nanowire sensor arrays. *Nat. Biotechnol.* **2005**, *23*, 1294–1301.
- (22) Stern, E.; Vacic, A.; Rajan, N. K.; Criscione, J. M.; Park, J.; Ilic, B. R.; Mooney, D. J.; Reed, M. A.; Fahmy, T. M. Label-free biomarker detection from whole blood. *Nat. Nanotechnol.* **2010**, *5*, 138–142.
- (23) Chua, J. H.; Chee, R. E.; Agarwal, A.; Wong, S. M.; Zhang, G. J. Label-free electrical detection of cardiac biomarker with complementary metal-oxide semiconductor-compatible silicon nanowire sensor arrays. *Anal. Chem.* **2009**, *81*, 6266–6271.
- (24) Horvath, I.; Hunt, J.; Barnes, P. J.; Alving, K. Exhaled breath condensate: methodological recommendations and unresolved questions. *Eur. Respir. J.* **2005**, *26*, 523–548.
- (25) Zakharkina, T.; Koczulla, A. R.; Mardanova, O.; Hattesoehl, A.; Bals, R. Detection of microorganisms in exhaled breath condensate during acute exacerbations of COPD. *Respirology* **2011**, *16*, 932–938.
- (26) Ikonen, N.; Strengell, M.; Kinnunen, L.; Österlund, P.; Pirhonen, J.; Broman, M.; Davidkin, I.; Ziegler, T.; Julkunen, I. High frequency of cross-reacting antibodies against 2009 pandemic influenza A(H1N1) virus among the elderly in Finland. *Euro Surveill.* **2010**, *15*, 19478.
- (27) Montuschi, P.; Collins, J. V.; Ciabattini, G.; Lazzeri, N.; Corradi, M.; Kharitonov, S. A.; Barnes, P. J. Exhaled 8-isoprostane as an in vivo biomarker of lung oxidative stress in patients with COPD and healthy smokers. *Am. J. Respir. Crit. Care Med.* **2000**, *162*, 1175–1177.
- (28) Centers for Disease Control and Prevention (2011). Guidance for Clinicians on the Use of Rapid Influenza Diagnostic Tests. http://www.cdc.gov/flu/professionals/diagnosis/clinician_guidance_ridt.htm (accessed Jan 1, 2012).